Inorg. Chem. **2008**, *47*, 4826−4831

Unique Structural Trends in the Lanthanoid Oxocarbonyl Complexes

Ling Jiang, Xin-Bo Zhang, Song Han, and Qiang Xu*

National Institute of Advanced Industrial Science and Technology (AIST), Ikeda, Osaka 563-8577, Japan

Received January 21, 2008

Reactions of laser-ablated lanthanoid atoms (except for radioactive Pm) with carbon dioxide molecules in solid argon have been investigated using matrix-isolation infrared spectroscopy. On the basis of isotopic shifts, mixed isotopic splitting patterns, and CCl_4-doping experiments, the lanthanoid oxocarbonyl complexes have been identified. Density functional theory calculations have been performed on these products, which support the experimental assignments of the infrared spectra. Infrared spectroscopic studies of these lanthanoid complexes combined with theoretical calculations reveal that the early lanthanoid (La−Sm) oxocarbonyl complexes adopt trans configurations, the europium and ytterbium ones adopt side-on-bonded modes (Eu-(η^2-OC)O and Yb-(η^2-OC)O), and the late lanthanoid (Gd−Lu) ones adopt cis configurations. Natural bond orbital analysis indicates that the formation of the lanthanoid oxocarbonyl complexes involves the promotion of 6s and 4f electrons into the metal valence shell.

Introduction

The synthesis and characterization of f-element metal complexes is one of the most challenging subjects in chemistry and has attracted much attention because of their applications in homogeneous catalysis, organic synthesis, and material science.[1] It is generally assumed that f-element chemistry exhibits monotonicity despite the variable electron counts and $4f^n$ configurations. For example, all of the tetrahydrofuran (THF) adducts of the lanthanoid complexes have similar structures, and their reactivities are also similar,[1b] which is quite different from the d-metals. In an alternative view, however, the special combination of the physical properties of the lanthanoid elements as large, highly electropositive metals with gradually changing size and limited orbital extension, provides the potential for proposing unique chemistry for these elements.

Interest in metal-mediated activation of carbon dioxide remains high because CO_2 doubles as an abundant renewable resource for the production of fine chemicals and clean fuels and a main contributor to global warming.[2] Extensive efforts have been made to recycle CO_2 from industrial emission and to remove some of this greenhouse gas.[2] Reactions of various metal atoms with carbon dioxide have been investigated, and a series of metal−carbon dioxide complexes have been experimentally characterized.[3–23] Quantum chemical calculations have been performed to understand the electronic

* To whom correspondence should be addressed. E-mail: q.xu@aist.go.jp.

(1) For example, see: (a) Evans, W. J. In *The Chemistry of the Metal−Carbon Bond*; Hartley, F. R., Patai, S., Eds.; Wiley: New York, 1982; Chapter 12. (b) Schumann, H.; Meese-Marktscheffel, J. A.; Esser, L. *Chem. Rev.* **1995**, *95*, 865. (c) Kaltsoyannis, N.; Scott, P. *The f Elements*; Oxford University Press: New York, 1999. (d) Li, J.; Bursten, B. E.; Liang, B.; Andrews, L. *Science* **2002**, *295*, 2242. (e) Dehnicke, K.; Greiner, A. *Angew. Chem., Int. Ed.* **2003**, *42*, 1340. (f) Castro-Rodriguez, I.; Nakai, H.; Zakharov, L. N.; Rheingold, A. L.; Meyer, K. *Science* **2004**, *305*, 1757. (g) Gottfriedsen, J.; Edelmann, F. T. *Coord. Chem. Rev.* **2007**, *251*, 142. (h) Evans, W. J. *Inorg. Chem.* **2007**, *46*, 3435. (i) Zhou, M. F.; Jin, X.; Gong, Y.; Li, J. *Angew. Chem., Int. Ed.* **2007**, *46*, 2911.

(2) For recent reviews, see: (a) Palmer, D. A.; van-Eldik, R. *Chem. Rev.* **1983**, *83*, 651. (b) Culter, A. R.; Hanna, P. K.; Vites, J. C. *Chem. Rev.* **1988**, *88*, 1363. (c) Jessop, P. G.; Ikariya, T.; Noyori, R. *Chem. Rev.* **1995**, *95*, 259. (d) Gibson, D. H. *Chem. Rev.* **1996**, *96*, 2063. (e) Gibson, D. H. *Coord. Chem. Rev.* **1999**, *185−186*, 335. (f) Oakes, R. S.; Clifford, A. A.; Rayner, C. M. *J. Chem. Soc., Perkin Trans. 1* **2001**, 917. (g) Leitner, W. *Acc. Chem. Res.* **2002**, *35*, 746. (h) Beckman, E. J. *J. Supercrit. Fluids* **2004**, *28*, 121. (i) Rayner, C. M. *Org. Process Res. Dev.* **2007**, *11*, 121.

(3) Kafafi, Z. H.; Hauge, R. H.; Billups, W. E.; Margrave, J. L. *J. Am. Chem. Soc.* **1983**, *105*, 3886 (Li + CO_2)

(4) Kafafi, Z. H.; Hauge, R. H.; Billups, W. E.; Margrave, J. L. *Inorg. Chem.* **1984**, *23*, 177 (Cs + CO_2)

(5) Andrews, L.; Tague, T. J., Jr. *J. Am. Chem. Soc.* **1998**, *120*, 13230 (Be + CO_2)

(6) Solov'ev, V. N.; Polikarpov, E. V.; Nemukhin, A. V.; Sergeev, G. B. *J. Phys. Chem. A* **1999**, *103*, 6721 (Mg + CO_2)

(7) Zhou, M. F.; Andrews, L. *J. Am. Chem. Soc.* **1998**, *120*, 13230 (Sc, Y + CO_2)

(8) (a) Mascetti, J.; Tranquille, M. *J. Phys. Chem.* **1988**, *92*, 2177. (b) Mascetti, J.; Galan, F.; Pàpai, I. *Coord. Chem. Rev.* **1999**, *190−192*, 557 (Ti, V, Cr, Fe, Co, Ni, Cu + CO_2). (c) Galan, F.; Fouassier, M.; Tranquille, M.; Mascetti, J.; Papai, I. *J. Phys. Chem. A* **1997**, *101*, 2626 (Ni + CO_2)

(9) Chertihin, G. V.; Andrews, L. *J. Am. Chem. Soc.* **1995**, *117*, 1595 (Ti + CO_2)

(10) Zhou, M. F.; Andrews, L. *J. Phys. Chem. A* **1999**, *103*, 2066 (Ti, V + CO_2)

10.1021/ic800112d CCC: $40.75
Published on Web 04/08/2008

structures and bonding characteristics of these complexes.[3–28] In contrast to the thermal-evaporation technique, the laser-ablation method produces more energetic atoms, allowing them to overpass energy barriers of some reactions.[3–23,29] In the laser-ablation experiments, for instance, insertion to produce OMCO has been observed for all the first-row transition metal atoms except Cu and Zn in the rare-gas matrices; the reactions of Cr through Cu atoms with CO_2 give the $OMCO^-$ anions, and Co, Ni, and Cu atoms also produce the addition MCO_2^- anions.[7,9–15] In contrast, insertion to produce OMCO has been observed only for the early transition metals (Sc−Cr), and all the other metals give $M(CO_2)$ complexes in the thermal experiments.[8]

Recent studies have shown that, with the aid of isotopic substitution, matrix isolation infrared spectroscopy, combined with quantum chemical calculation, is very powerful in the investigation of the spectra, structure, and bonding of novel species.[30,31] In contrast with the extensive experimental and theoretical studies of the interactions of CO_2 molecules with the transition metal and main group element atoms in the matrix experiments,[3–23] much less work has been done on the interaction of carbon dioxide with the lanthanoid elements (Ln). Recently, kinetic studies of gas-phase lanthanoid atoms with CO_2 reveal that the lanthanoid atoms, except Yb, abstract an oxygen atom to produce the metal oxide.[32–34] Herein, we report a systematical study of the reactions of CO_2 with Ln atoms. Matrix-isolation infrared spectroscopy, coupled with theoretical calculation, provides obvious evidence for the formation of the lanthanoid oxocarbonyl complexes, which reveal a unique structural trend in lanthanoid−ligand interactions.

Experimental and Theoretical Methods

The experiment for laser-ablation and matrix-isolation infrared spectroscopy is similar to those previously reported.[35,36] In short, the Nd:YAG laser fundamental (1064 nm, 10 Hz repetition rate with 10 ns pulse width) was focused on the rotating lanthanoid (except for radioactive Pm) targets. The laser-ablated Ln atoms were codeposited with CO_2 in excess argon onto a CsI window cooled normally to 4 K by means of a closed-cycle helium refrigerator. Typically, 1−20 mJ/pulse laser power was used. CO_2 (99.99%, Takachiho Chemical Industrial Co., Ltd.), $^{13}C^{16}O_2$ (99%, ^{18}O < 1%, Cambridge Isotopic Laboratories), $^{12}C^{18}O_2$ (95%, Cambridge Isotopic Laboratories), $^{12}C^{16}O_2 + {}^{13}C^{16}O_2$, and $^{12}C^{16}O_2 + {}^{12}C^{18}O_2$ were used in different experiments. In general, matrix samples were deposited for 30 to 60 min with a typical rate of 2−4 mmol per hour. After sample deposition, IR spectra were recorded on a BIO-RAD FTS-6000e spectrometer at 0.5 cm^{-1} resolution using a liquid-nitrogen-cooled HgCdTe (MCT) detector for the spectral range of 5000−400 cm^{-1}. Samples were annealed at different temperatures and subjected to broadband irradiation (λ > 250 nm) using a high-pressure mercury arc lamp (Ushio, 100 W).

DFT calculations were performed to predict the structures and vibrational frequencies of the observed reaction products using the Gaussian 03 program.[37] The B3LYP density functional method was

(11) Zhang, L.; Wang, X.; Chen, M.; Qin, Q. Z *Chem. Phys.* **2000**, *254*, 231 (Zr + CO_2)

(12) Chen, M.; Wang, X.; Zhang, L.; Qin, Q. Z. *J. Phys. Chem. A* **2000**, *104*, 7010 (Nb + CO_2)

(13) Wang, X.; Chen, M.; Zhang, L.; Qin, Q. Z. *J. Phys. Chem. A* **2000**, *104*, 758 (Ta + CO_2)

(14) (a) Souter, P. F.; Andrews, L. *Chem. Commun.* **1997**, 777. (b) Souter, P. F.; Andrews, L. *J. Am. Chem. Soc.* **1997**, *119*, 7350 (Cr, Mo, W + CO_2)

(15) Zhou, M. F.; Liang, B.; Andrews, L. *J. Phys. Chem. A* **1999**, *103*, 2013 (Cr−Zn + CO_2)

(16) Liang, B.; Andrews, L. *J. Phys. Chem. A* **2002**, *106*, 595 (Re + CO_2)

(17) Liang, B.; Andrews, L. *J. Phys. Chem. A* **2002**, *106*, 4042 (Os, Ru + CO_2)

(18) Andrews, L.; Zhou, M. F.; Liang, B.; Li, J.; Bursten, B. E. *J. Am. Chem. Soc.* **2000**, *122*, 11440 (U, Th + CO_2)

(19) Bulkholder, T. R.; Andrews, L.; Bartlett, R. J. *J. Phys. Chem.* **1993**, *97*, 3500 (B + CO_2)

(20) Quere, A. M. L.; Xu, C.; Manceron, L. *J. Phys. Chem.* **1991**, *95*, 3031 (Al + CO_2)

(21) Brock, L. R.; Duncan, M. A. *J. Phys. Chem.* **1991**, *95*, 3031 (Al + CO_2)

(22) Howard, J. A.; McCague, C.; Sutcliffe, R.; Tse, J. S.; Joly, H. A. *J. Chem. Soc., Faraday Trans.* **1995**, *91*, 799 (Al, Ga + CO_2)

(23) Himmel, H. J.; Downs, A. J.; Greene, T. M. *Chem. Rev.* **2002**, *102*, 4191 and references therein.

(24) (a) Sodupe, M.; Branchadell, V.; Oliva, A. *J. Phys. Chem.* **1995**, *99*, 8567. (b) Hwang, D. Y.; Mebel, A. M. *Chem. Phys. Lett.* **2002**, *357*, 51. (c) Papai, I.; Schubert, G.; Hannachi, Y.; Mascetti, J. *J. Phys. Chem. A* **2002**, *106*, 9551 (Sc + CO_2)

(25) (a) Papai, I.; Mascetti, J.; Fournier, R. *J. Phys. Chem. A* **1997**, *101*, 4465. (b) Hwang, D. Y.; Mebel, A. M. *J. Chem. Phys.* **2002**, *116*, 5633 (Ti + CO_2)

(26) Papai, I.; Hannachi, Y.; Gwizdala, S.; Mascetti, J. *J. Phys. Chem. A* **2002**, *106*, 4181 (V + CO_2)

(27) (a) Mebel, A. M.; Hwang, D. Y. *J. Phys. Chem. A* **2000**, *104*, 11622. (b) Hannachi, Y.; Mascetti, J.; Stirling, A.; Papai, I. *J. Phys. Chem. A* **2003**, *107*, 6708 (Ni + CO_2)

(28) Dobrogorskaya, Y.; Mascetti, J.; Papai, I.; Hannachi, Y. *J. Phys. Chem. A* **2005**, *109*, 7932 (Cu + CO_2)

(29) Liu, X. J.; Zhang, X.; Han, K. L.; Xing, X. P.; Sun, S. T.; Tang, Z. C. *J. Phys. Chem. A* **2007**, *111*, 3248.

(30) For example, see: (a) Xu, C.; Manceron, L.; Perchard, J. P. *J. Chem. Soc., Faraday Trans.* **1993**, *89*, 1291. (b) Bondybey, V. E.; Smith, A. M.; Agreiter, J. *Chem. Rev.* **1996**, *96*, 2113. (c) Fedrigo, S.; Haslett, T. L.; Moskovits, M. *J. Am. Chem. Soc.* **1996**, *118*, 5083. (d) Khriachtchev, L.; Pettersson, M.; Runeberg, N.; Lundell, J.; Rasanen, M. *Nature* **2000**, *406*, 874. (e) Himmel, H. J.; Manceron, L.; Downs, A. J.; Pullumbi, P. *J. Am. Chem. Soc.* **2002**, *124*, 4448. (f) Andrews, L.; Wang, X. *Science* **2003**, *299*, 2049.

(31) (a) Zhou, M. F.; Tsumori, N.; Li, Z.; Fan, K.; Andrews, L.; Xu, Q. *J. Am. Chem. Soc.* **2002**, *124*, 12936. (b) Zhou, M. F.; Xu, Q.; Wang, Z.; von Ragué Schleyer, P. *J. Am. Chem. Soc.* **2002**, *124*, 14854. (c) Jiang, L.; Xu, Q. *J. Am. Chem. Soc.* **2005**, *127*, 42. (d) Xu, Q.; Jiang, L.; Tsumori, N. *Angew. Chem., Int. Ed.* **2005**, *44*, 4338. (e) Jiang, L.; Xu, Q. *J. Am. Chem. Soc.* **2005**, *127*, 8906.

(32) Campbell, M. L. *Phys. Chem. Chem. Phys.* **1999**, *1*, 3731 (La−Yb + CO_2 in the gas phase)

(33) Campbell, M. L. *Chem. Phys. Lett.* **2000**, *330*, 547 (Lu + CO_2 in the gas phase)

(34) Larsson, R.; Mascetti, J. *React. Kinet. Catal. Lett.* **2005**, *85*, 107 (Ln + CO_2 in the gas phase)

(35) Burkholder, T. R.; Andrews, L. *J. Chem. Phys.* **1991**, *95*, 8697.

(36) (a) Zhou, M. F.; Tsumori, N.; Andrews, L.; Xu, Q. *J. Phys. Chem. A* **2003**, *107*, 2458. (b) Jiang, L.; Xu, Q. *J. Chem. Phys.* **2005**, *122*, 034505. (c) Jiang, L.; Teng, Y. L.; Xu, Q. *J. Phys. Chem. A* **2006**, *110*, 7092.

(37) Frisch, M. J.; Trucks, G. W.; Schlegel, H. B.; Scuseria, G. E.; Robb, M. A.; Cheeseman, J. R.; Montgomery, J. A., Jr.; Vreven, T.; Kudin, K. N.; Burant, J. C.; Millam, J. M.; Iyengar, S. S.; Tomasi, J.; Barone, V.; Mennucci, B.; Cossi, M.; Scalmani, G.; Rega, N.; Petersson, G. A.; Nakatsuji, H.; Hada, M.; Ehara, M.; Toyota, K.; Fukuda, R.; Hasegawa, J.; Ishida, M.; Nakajima, T.; Honda, Y.; Kitao, O.; Nakai, H.; Klene, M.; Li, X.; Knox, J. E.; Hratchian, H. P.; Cross, J. B.; Adamo, C.; Jaramillo, J.; Gomperts, R.; Stratmann, R. E.; Yazyev, O.; Austin, A. J.; Cammi, R.; Pomelli, C.; Ochterski, J. W.; Ayala, P. Y.; Morokuma, K.; Voth, G. A.; Salvador, P.; Dannenberg, J. J.; Zakrzewski, V. G.; Dapprich, S.; Daniels, A. D.; Strain, M. C.; Farkas, O.; Malick, D. K.; Rabuck, A. D.; Raghavachari, K.; Foresman, J. B.; Ortiz, J. V.; Cui, Q.; Baboul, A. G.; Clifford, S.; Cioslowski, J.; Stefanov, B. B.; Liu, G.; Liashenko, A.; Piskorz, P.; Komaromi, I.; Martin, R. L.; Fox, D. J.; Keith, T.; Al-Laham, M. A.; Peng, C. Y.; Nanayakkara, A.; Challacombe, M.; Gill, P. M. W.; Johnson, B.; Chen, W.; Wong, M. W.; Gonzalez, C.; Pople, J. A. *Gaussian 03*, revision B.04; Gaussian, Inc.: Pittsburgh, PA, 2003.

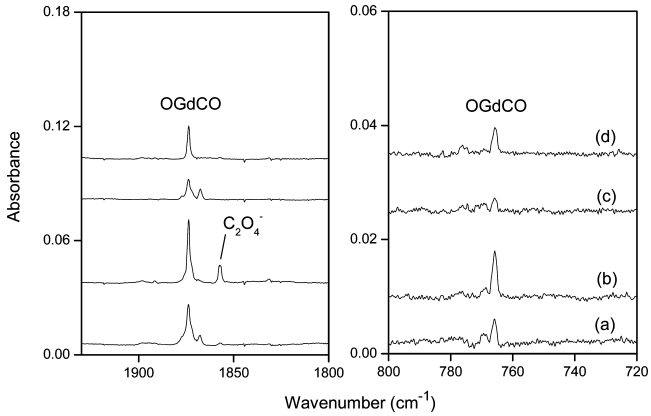

Figure 1. Infrared spectra in the 1900−1800 and 800−720 cm^{-1} regions from codeposition of laser-ablated Gd atoms with 0.5% CO_2 in Ar: (a) 1 h of sample deposition at 4 K, (b) after annealing to 25 K, (c) after 15 min of broadband irradiation, and (d) after annealing to 30 K.

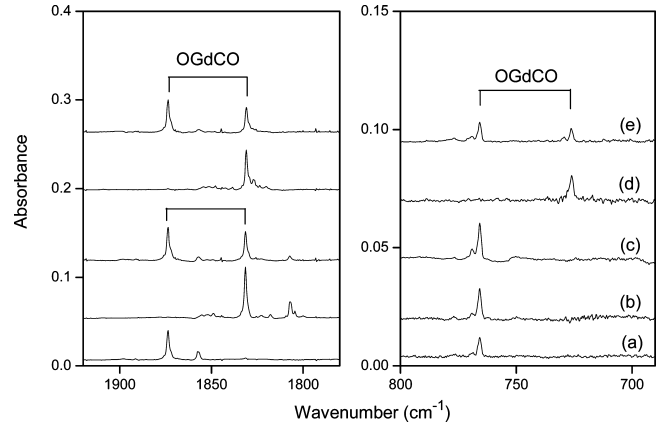

Figure 2. Infrared spectra in the 1900−1800 and 800−700 cm^{-1} regions from codeposition of laser-ablated Gd atoms with isotopic CO_2 in Ar after annealing to 25 K: (a) 0.5% $^{12}C^{16}O_2$, (b) 0.5% $^{13}C^{16}O_2$, (c) 0.3% $^{12}C^{16}O_2$ + 0.3% $^{13}C^{16}O_2$, (d) 0.5% $^{12}C^{18}O_2$, and (e) 0.3% $^{12}C^{16}O_2$ + 0.3% $^{12}C^{18}O_2$.

used.[38] The Aug-cc-pVQZ basis set was used for the C and O atoms,[39] and the scalar-relativistic SDD pseudopotential and basis sets were used for the Ln atoms.[40] Geometries were fully optimized and vibrational frequencies were calculated with analytical second derivatives. The natural bond orbital (NBO)[41] approach was employed to elucidate the electron configuration and the bonding characteristics. Trial calculations and recent investigations have shown that such computational methods can provide reliable information for the lanthanoid complexes, such as infrared frequencies, relative absorption intensities, and isotopic shifts.[42] Molecular orbitals were generated with GaussView.

Results and Discussion

Experiments have been done with carbon dioxide concentrations ranging from 0.02% to 2.0% in excess argon. Typical infrared spectra for the reactions of laser-ablated Gd, Nd, and Eu atoms with CO_2 molecules in excess argon in the selected regions are illustrated in Figures 1–4. The spectra of the other lanthanoid elements are shown as Supporting Information.[43] The absorption bands in different isotopic experiments are listed in Table 1. The IR spectra of the La + CO_2 reaction have been reported previously,[44] and only the absorption bands of OLaCO are listed here (Table 1). Doping with CCl_4 as an electron scavenger has no effect on these bands, indicating that the products are neutral (not shown here).[45]

Quantum chemical calculations have been carried out for the possible isomers and electronic states of the lanthanoid oxocarbonyl complexes. Optimized molecular structures of the potential products are illustrated in Figure 5, and the geometric parameters of these complexes are given in Table 2. Natural electron configurations of lanthanoid atoms in the lanthanoid oxocarbonyl complexes are listed in Table 3. Table S1 reports a comparison of observed and calculated IR frequencies for the lanthanoid oxocarbonyl complexes.[43]

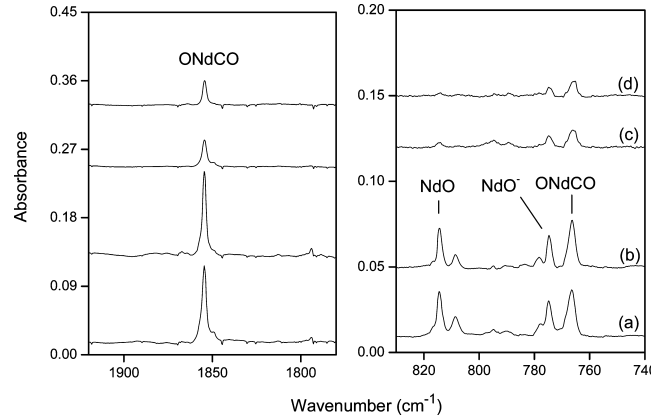

Figure 3. Infrared spectra in the 1900−1800 and 820−740 cm^{-1} regions from codeposition of laser-ablated Nd atoms with 0.5% CO_2 in Ar: (a) 45 min of sample deposition at 4 K, (b) after annealing to 25 K, (c) after 12 min of broadband irradiation, and (d) after annealing to 30 K.

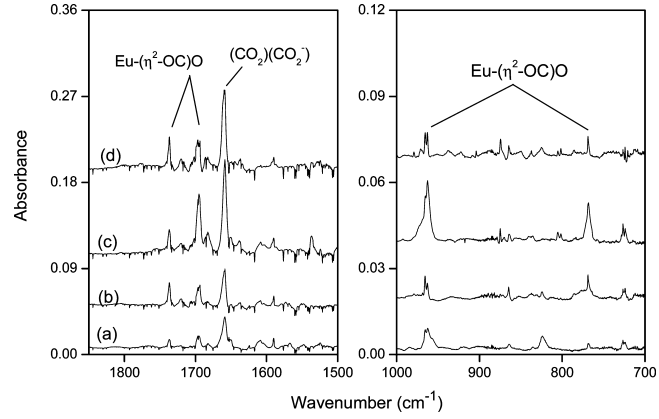

Figure 4. Infrared spectra in the 1800−1500 and 1000−700 cm^{-1} regions from codeposition of laser-ablated Eu atoms with 0.8% CO_2 in Ar: (a) 45 min of sample deposition at 4 K, (b) after annealing to 25 K, (c) after 10 min of broadband irradiation, and (d) after annealing to 30 K.

(38) (a) Lee, C.; Yang, E.; Parr, R. G. *Phys. Rev. B* **1988**, *37*, 785. (b) Becke, A. D. *J. Chem. Phys.* **1993**, *98*, 5648.
(39) (a) Dunning, T. H., Jr. *J. Chem. Phys.* **1989**, *90*, 1007. (b) Kendall, R. A.; Dunning, T. H., Jr.; Harrison, R. J. *J. Chem. Phys.* **1992**, *96*, 6796.
(40) (a) Dolg, M.; Stoll, H.; Preuss, H. *J. Chem. Phys.* **1989**, *90*, 1730. (b) Cao, X.; Dolg, M. *J. Chem. Phys.* **2001**, *115*, 7348.
(41) Glendening, E. D.; Reed, A. E.; Carpenter, J. E.; Weinhold. F. *NBO*, version 3.1; University of Wisconsin: Madison, WI, 1995.
(42) (a) Xu, J.; Zhou, M. F. *J. Phys. Chem. A* **2006**, *110*, 10575. (b) Xu, J.; Jin, X.; Zhou, M. F. *J. Phys. Chem. A* **2007**, *111*, 7105. (c) Hirva, P.; Haukka, M.; Jakonen, M.; Moreno, M. A. *J. Mol. Model* **2008**, *14*, 171.
(43) See Supporting Information.
(44) Jiang, L.; Xu, Q. *J. Phys. Chem. A* **2007**, *111*, 3519 (La + CO_2)
(45) Zhou, M. F.; Andrews, L., Jr. *Chem. Rev.* **2001**, *101*, 1931.

Table 1. Absorptions (in cm^{-1}) Observed from Codeposition of Laser-Ablated Ln Atoms with CO_2 in Excess Argon at 4 K

$^{12}C^{16}O_2$	$^{13}C^{16}O_2$	$^{12}C^{18}O_2$	R(12/13)	R(16/18)	species
1839.9	1798.8	1797.4	1.0228	1.0236	OLaCO
753.6	753.6	714.9	1.0000	1.0541	
1845.6	1804.4	1803.1	1.0228	1.0236	OCeCO
737.0	737.0	699.6	1.0000	1.0535	
1846.8	1805.6	1804.4	1.0228	1.0235	OPrCO
776.0	766.0	736.5	1.0000	1.0401	
1854.5	1812.7	1811.6	1.0231	1.0237	ONdCO
766.3	766.3	727.7	1.0000	1.0530	
1854.6	1814.0	1812.6	1.0224	1.0232	OSmCO
749.2	749.0	710.7	1.0003	1.0542	
1692.2	1640.8	1658.8	1.0313	1.0201	Eu-(η^2-OC)O
962.8	951.1	919.5	1.0123	1.0471	
768.9	758.5	741.1	1.0137	1.0375	
1873.7	1831.4	1830.9	1.0231	1.0234	OGdCO
765.7	765.7	726.1	1.0000	1.0545	
1868.5	1826.2	1826.3	1.0232	1.0231	OTbCO
779.1	779.1	738.8	1.0000	1.0545	
1864.9	1822.5	1822.9	1.0233	1.0230	ODyCO
787.4	787.4	747.0	1.0000	1.0541	
1869.1	1826.5	1827.1	1.0233	1.0230	OHoCO
787.9	787.9	748.3	1.0000	1.0529	
1873.3	1830.6	1831.3	1.0233	1.0229	OErCO
787.8	787.8	747.0	1.0000	1.0547	
1868.5	1825.8	1826.9	1.0234	1.0228	OTmCO
788.5	788.5	747.8	1.0000	1.0544	
1740.6	1696.9	1703.3	1.0258	1.0219	Yb-(η^2-OC)O
957.2	947.9	906.1	1.0098	1.0564	
777.5	770.3	742.3	1.0093	1.0474	
1875.5	1832.5	1833.9	1.0235	1.0227	OLuCO
798.4	797.9	756.6	1.0006	1.0552	

Molecular orbital pictures of the lanthanoid oxocarbonyl complexes showing the highest occupied molecular orbitals (HOMO) down to the third valence molecular orbital from the HOMO are illustrated in Figure S23.[43]

A. Identification of Lanthanoid Oxocarbonyl Complexes. For the reactions of CO_2 with Ln atoms, except for Eu and Yb, two classes of major new features in the 1900−1800 and 810−720 cm^{-1} regions have been observed (Table 1, and Figures 1, 2, and S1−S22[43]). Taking the Gd reaction as an example, two absorptions at 1873.7 and 765.7 cm^{-1} appear together during sample deposition, increase after sample annealing to 25 K, decrease upon broadband irradiation, and recover after further annealing to higher temperature (Figure 1). The upper band of 1873.7 cm^{-1} shifts to 1831.4 cm^{-1} with $^{13}C^{16}O_2$ and to 1830.9 cm^{-1} with $^{12}C^{18}O_2$, exhibiting isotopic frequency ratios ($^{12}C^{16}O_2/^{13}C^{16}O_2$, 1.0231; $^{12}C^{16}O_2/^{12}C^{18}O_2$, 1.0234) characteristic of C−O stretching vibrations. The mixed $^{12}C^{16}O_2 + {}^{13}C^{16}O_2$ and $^{12}C^{16}O_2 + {}^{12}C^{18}O_2$ isotopic spectra (Figure 2, traces c and e) only provide the sum of pure isotopic bands, which indicates that only one CO unit is involved in this carbonyl stretching mode.[46] The 765.7 cm^{-1} band shows no carbon isotopic shift but shifts to 726.1 cm^{-1} with $^{12}C^{18}O_2$. The $^{12}C^{16}O_2/^{12}C^{18}O_2$ isotopic frequency ratio of 1.0545 is very close to the diatomic $Gd^{16}O/Gd^{18}O$ frequency ratio of 1.0542,[47] suggesting a Gd−O stretching mode. Only doublets have been observed in the $^{12}C^{16}O_2 + {}^{12}C^{18}O_2$ isotopic spectra (Figure 2, trace e). The absorptions at 1873.7 and 765.7 cm^{-1} are therefore assigned to the C−O and Gd−O stretching vibrations of the neutral OGdCO complex.

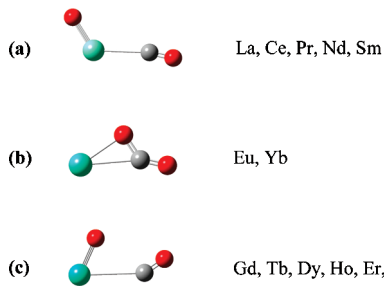

Figure 5. Optimized molecular structures of the potential products. The geometric parameters of these complexes are given in Table 2.

The present calculations predict that OGdCO has a C_s symmetry with a $^9A''$ ground state (Table 2 and Figure 5). For the C−O stretching mode, the vibrational frequency is calculated at 2199.7 cm^{-1}, which should be scaled down by 0.8518 to fit the experimental frequency. The $^{12}C^{16}O_2/^{13}C^{16}O_2$ and $^{12}C^{16}O_2/^{12}C^{18}O_2$ isotopic frequency ratios of 1.0230 and 1.0243 (Table S1)[43] are consistent with the experimental values of 1.0231 and 1.0234, respectively. The calculated Gd−O stretching vibration (777.1 cm^{-1}) and the $^{12}C^{16}O_2/^{12}C^{18}O_2$ isotopic frequency ratio (1.0547) are in good agreement with the experimental values (Table S1),[43] respectively. The deviations for the C−O stretching vibrational frequencies from the experimental values are 98.1 (La), 93.8 (Ce), 112.0 (Pr), 100.3 (Nd), 162.5 (Sm), 326.0 (Gd), 345.1 (Tb), 311.7 (Dy), 327.7 (Ho), 318.3 (Er), 278.7 (Tm), and 296.9 cm^{-1} (Lu) (Table S1),[43] respectively, whereas those for the Ln−O stretching vibrational frequencies are smaller (0.5−68.5 cm^{-1}). Such large deviations for the C−O stretching vibrational frequencies of the lanthanoid carbonyls may be caused by the inefficiency of the XC functional or the basis sets used here, posing a formidable theoretical challenge because of the large numbers of f-electrons and strong relativistic effects.[48–51]

The reactions of CO_2 with Eu and Yb produce the Eu-(η^2-OC)O and Yb-(η^2-OC)O complexes, which show lower C−O stretching vibrations. Taking the Eu reaction as an example, three absorptions at 1692.2, 962.8, and 768.9 cm^{-1} appear together during sample deposition, increase slightly after sample annealing to 25 K, and increase visibly upon broadband irradiation and after further annealing to higher temperature (Figure 4). The absorption at 1692.2 cm^{-1} shifts to 1640.8 cm^{-1} with $^{13}C^{16}O_2$ and to 1658.8 cm^{-1} with $^{12}C^{18}O_2$, exhibiting isotopic frequency ratios ($^{12}C^{16}O_2/^{13}C^{16}O_2$, 1.0313; $^{12}C^{16}O_2/^{12}C^{18}O_2$, 1.0201) characteristic of C−O stretching vibrations (Table 1). The mixed $^{12}C^{16}O_2 + {}^{13}C^{16}O_2$ isotopic spectra (Figure S8)[43] only provide the sum of pure isotopic bands, indicating that only one CO unit is involved in this carbonyl stretching mode.[46] The absorptions at 962.8 and 768.9 cm^{-1} shift to 951.1 and 758.5 cm^{-1} with $^{13}C^{16}O_2$

(46) Darling, J. H.; Ogden, J. S. *J. Chem. Soc., Dalton Trans.* **1972**, 2496.
(47) (a) Willson, S. P.; Andrews, L. *J. Phys. Chem. A* **1999**, *103*, 3171. (b) Willson, S. P.; Andrews, L. *J. Phys. Chem. A* **1999**, *103*, 6972.
(48) For example, see: (a) Pyykkö, P. *Chem. Rev.* **1988**, *88*, 563. (b) Pepper, M.; Bursten, B. E. *Chem. Rev.* **1991**, *91*, 719. (c) Seth, M.; Dolg, M.; Fulde, P.; Schwerdtfeger, P. *J. Am. Chem. Soc.* **1995**, *117*, 6597. (d) Li, J.; Bursten, B. E. *J. Am. Chem. Soc.* **1997**, *119*, 9021.
(49) (a) Adamo, C.; Maldivi, P. *J. Phys. Chem. A* **1998**, *102*, 6812. (b) Dolg, M.; Liu, W.; Kalvoda, S. *Int. J. Quantum Chem.* **2000**, *76*, 359. (c) Maron, L.; Eisenstein, O. *J. Phys. Chem. A* **2000**, *104*, 7140.
(50) Gibson, J. K. *J. Phys. Chem. A* **2003**, *107*, 7891.
(51) de Almeida, K. J.; Cesar, A. *Organometallics* **2006**, *25*, 3407.

Table 2. Molecular Structures, Electronic States, and Geometries Calculated for the Lanthanoid Oxocarbonyl Complexes

species	structure	electronic state	geometry					
			d_{O-Ln}	d_{Ln-C}	d_{C-O}	∠OLnC	∠LnCO	∠OCO
OLaCO	C_s	$^2A''$	1.849	2.576	1.157	110.6	179.2	
OCeCO	C_s	$^3A''$	1.831	2.516	1.158	110.8	179.3	
OPrCO	C_s	$^4A''$	1.831	2.497	1.155	114.4	177.6	
ONdCO	C_s	$^5A''$	1.825	2.494	1.155	108.9	176.9	
OSmCO	C_s	$^7A''$	1.863	2.636	1.141	123.6	169.0	
Eu-(η^2-OC)O	C_s	$^8A''$	2.257	2.585	1.191	29.8	163.5	135.7
OGdCO	C_s	$^9A''$	1.843	3.010	1.124	64.4	146.9	
OTbCO	C_s	$^8A''$	1.787	3.305	1.123	70.9	142.2	
ODyCO	C_s	$^5A''$	1.856	2.749	1.127	63.4	154.4	
OHoCO	C_s	$^4A''$	1.833	2.627	1.124	66.4	158.1	
OErCO	C_s	$^3A''$	1.831	2.601	1.125	66.3	157.9	
OTmCO	C_s	$^2A''$	1.860	2.514	1.130	61.9	159.9	
Yb-(η^2-OC)O	C_s	$^1A'$	2.208	2.477	1.185	30.9	158.3	138.9
OLuCO	C_s	$^2A'$	1.828	2.497	1.127	64.2	159.9	

Table 3. Natural Electron Configurations of Lanthanoid Atoms in the Lanthanoid Oxocarbonyl Complexes

atom	natural electron configuration
La	[core] 6s(0.05) 4f(0.15) 5d(0.78) 6p(0.04) 5f(0.01)
Ce	[core] 6s(0.05) 4f(1.20) 5d(0.79) 6p(0.04) 5f(0.01)
Pr	[core] 6s(0.05) 4f(2.28) 5d(0.75) 6p(0.04)
Nd	[core] 6s(0.05) 4f(3.25) 5d(0.77) 6p(0.04)
Sm	[core] 6s(0.05) 4f(5.71) 5d(0.48) 6p(0.05)
Eu	[core] 6s(0.96) 4f(6.99) 5d(0.14)
Gd	[core] 6s(0.96) 4f(7.04) 5d(0.55) 6p(0.05) 7s(0.02)
Tb	[core] 6s(1.39) 4f(7.32) 5d(0.58) 6p(0.07) 7s(0.33)
Dy	[core] 6s(0.99) 4f(8.89) 5d(0.50) 6p(0.04) 7s(0.15)
Ho	[core] 6s(0.88) 4f(10.18) 5d(0.47) 6p(0.05)
Er	[core] 6s(0.92) 4f(11.13) 5d(0.48) 6p(0.05)
Tm	[core] 6s(0.71) 4f(12.40) 5d(0.38) 6p(0.05)
Yb	[core] 6s(1.13) 4f(13.97) 5d(0.10)
Lu	[core] 6s(0.98) 5d(0.80) 6p(0.03) 6d(0.01)

and to 919.5 and 741.1 cm^{-1} with $^{12}C^{18}O_2$. The very low C−O stretching vibrational frequency of 1692.2 cm^{-1} is reminiscent of the side-on-bonded structure of the M-(η^2-OC)O (M = Sc, Y) complexes, in which the corresponding frequencies have been observed at 1763.4 and 1773.1 cm^{-1} in the previous argon matrix experiments, respectively.[7] Accordingly, the 1692.2, 962.8, and 768.9 cm^{-1} bands are assigned to the antisymmetric O−C−O, symmetric O−C−O stretching, and O−C−O bending vibrational modes of the Eu-(η^2-OC)O complex, respectively. The corresponding absorptions of the analogous Yb-(η^2-OC)O complex have been observed at 1740.6, 957.2, and 777.5 cm^{-1} (Table 1), respectively.

DFT calculations have been performed for the Eu-(η^2-OC)O and Yb-(η^2-OC)O complexes, and these support the above assignments. The Eu-(η^2-OC)O and Yb-(η^2-OC)O complexes are predicted to have a C_s symmetry with the $^8A''$ and $^1A''$ ground states (Table 2 and Figure 5), respectively. The antisymmetric O−C−O stretching vibrational frequency in the Eu-(η^2-OC)O complex is calculated at 1812.9 cm^{-1} with $^{12}C^{16}O_2/^{13}C^{16}O_2$ and $^{12}C^{16}O_2/^{12}C^{18}O_2$ isotopic frequency ratios of 1.0257 and 1.0203 (Table S1),[43] which are consistent with the experimental observations. Similar agreements have also been obtained for the Yb-(η^2-OC)O complex.

It can be seen from the IR spectra (Figures 1, 3, 4, and S1−S22[43]) that the behavior with annealing or photochemistry is not the same for all the metals. The absorptions of oxocarbonyl complexes for Eu through Lu visibly increase after sample annealing, whereas those for the early lanthanoid oxocarbonyl complexes (La−Sm) change little after annealing. Upon broadband irradiation, the bands grow for Eu and Yb, whereas CO detachment was observed for the other metals. These findings suggest that the early lanthanoid atoms are more reactive with CO_2 than the late ones, followed by Eu and Yb. Gas-phase reactions of lanthanoid atoms with CO_2 show that with the exception of Yb, the lanthanoids abstract an oxygen atom to yield the metal oxide; energy barriers increase generally from the left to the right side of the lanthanoids.[32] Detailed calculations on the potential energy surface along the reactions of lanthnoid atoms with CO_2 are underway and will be reported in a subsequent paper.

B. Structural Trends. The identification of the lanthanoid oxocarbonyl complexes has been discussed in the above section. We turn now to general trends in the interaction of carbon dioxide with the lanthanoid atoms. We can roughly draw two lines based on the experimental values (Figure 6); one involves Eu and Yb, and another one involves the other lanthanoid atoms. The vibrational frequencies on the upper line show small changes and a general increase along the series, providing an example of the effects of lanthanoid contraction.[48–51] This trend holds true for the calculated C−O stretching frequencies (Table S1).[43]

The geometry optimization of the lanthanoid oxocarbonyl complexes spanning the lanthanoid series gives three dif-

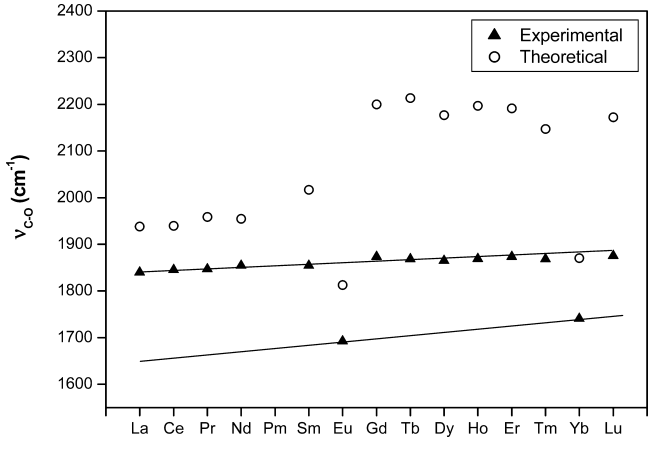

Figure 6. Plot of the experimental and theoretically calculated C−O stretching frequencies (cm^{-1}) in the lanthanoid oxocarbonyl complexes. Two lines are roughly drawn for the experimental values.

ferent kinds of geometrical structures (Figure 5): (**a**) the early lanthanoid oxocarbonyl complexes (La, Ce, Pr, Nd, Sm) adopt the trans configurations; (**b**) the europium and ytterbium oxocarbonyl complexes adopt side-on-bonded modes (Eu-(η^2-OC)O and Yb-(η^2-OC)O); (**c**) the late lanthanoid oxocarbonyl complexes (Gd, Tb, Dy, Ho, Er, Tm, Lu) adopt the cis configurations. Molecular orbital analysis[43] shows that the HOMOs down to the third valence molecular orbitals of the lanthanoid oxocarbonyl complexes of kind **a** are almost the same. Similar results have also been obtained for the oxocarbonyl complexes of kind **b**. For the oxocarbonyl complexes of kind **c**, the HOMO-2s are the same. In contrast, the most stable isomers of OMCO with cis configurations have been observed for all the first-row transition metal atoms except Cu and Zn and the $OMCO^-$ intersection molecular anions for all the first-row transition metal atoms in the laser-ablation experiments,[7,9–15] different from the structural trends in the lanthanoid oxocarbonyl complexes.

The role of the 4f orbitals in the chemical bonds of lanthanoid complexes has been a matter of current theoretical investigations.[49–51] In general, the 4f orbitals do not contribute appreciably either to the bonding or to the antibonding molecular orbitals, and therefore, the lanthanoids should form chemical bonds almost exclusively by sharing their 6s5d hybrid atomic orbitals. In this work, NBO analysis results indicate that there are some electrons in the 5d and 6p orbitals of Ln atoms except for Eu and Yb in the oxocarbonyl complexes, whereas no electron has been observed in the 6p orbitals in the Eu and Yb (Table 3). This implies that the formation of the lanthanoid (except for Eu and Yb) oxocarbonyl complexes involves the promotion of 6s and 4f electrons into the metal valence shell. The Eu and Yb atoms have very stable $4f^76s^2$ and $4f^{14}6s^2$ electron configurations, respectively, which hardly promote f electrons into the metal valence shell. The 6s electrons in the Eu and Yb atoms have been promoted to the 5d orbitals. The NBO analyses further reveal that the lanthanoid (except for Eu and Yb) oxocarbonyl complexes have significant bonding interactions between the O 2p orbitals and the Ln 5d orbitals, whereas the Eu and Yb ones have significant bonding interactions between the C 2p orbitals and the Eu and Yb 6s orbitals, exhibiting the difference in chemistry between the semifilled-f-orbital Eu/full-filled-f-orbital Yb and the other lanthanoid elements. Further calculations to make clear the structural difference in the lanthanoid oxocarbonyl complexes are in progress.

Conclusions

We have demonstrated that infrared spectroscopy of the lanthanoid oxocarbonyl complexes in the C−O stretching region, combined with DFT calculations, provides significant structural insights into the interaction of carbon dioxide with the lanthanoid elements. The early lanthanoid (La−Sm) oxocarbonyl complexes adopt trans configurations, the europium and ytterbium ones adopt side-on-bonded modes (Eu-(η^2-OC)O and Yb-(η^2-OC)O), and the late lanthanoid (Gd−Lu) ones adopt cis configurations. Note that the calculation of the lanthanoid complexes poses a formidable theoretical challenge, due to the large numbers of f-electrons and strong relativistic effects. It is possible that further development in the necessary theoretical tools for the lanthanoid elements, through matrix-isolation investigations, will lead to new discoveries of interesting aspects in lanthanoid chemistry.

Acknowledgment. This work was supported by AIST and a Grant-in-Aid for Scientific Research (B) (Grant No. 17350012) from the Ministry of Education, Culture, Sports, Science and Technology (MEXT) of Japan. L.J. is grateful to JSPS for a postdoctoral fellowship.

Supporting Information Available: Comparison of observed and calculated IR frequencies for the lanthanoid oxocarbonyl complexes; infrared spectra of the Ce, Pr, Nd, Sm, Eu, Tb, Dy, Ho, Er, Tm, Yb, and Lu reactions; and molecular orbital pictures of the lanthanoid oxocarbonyl complexes. This material is available free of charge via the Internet at http://pubs.acs.org.

IC800112D